Pressure effect and superconductivity in the β-Bi_4I_4 topological insulator

A. Pisoni,[1,*] R. Gaál,[1] A. Zeugner,[2] V. Falkowski,[3] A. Isaeva,[2] H. Huppertz,[3] G. Autès,[1] O. V. Yazyev,[1] and L. Forró[1]

[1]*Institute of Physics, Ecole Polytechnique Fédérale de Lausanne (EPFL), CH-1015 Lausanne, Switzerland*

[2]*Department of Chemistry and Food Chemistry, TU Dresden, D-01062 Dresden, Germany*

[3]*Institute of General, Inorganic and Theoretical Chemistry, University of Innsbruck, A-6020 Innsbruck, Austria*

(Received 15 February 2017; revised manuscript received 16 April 2017; published 26 June 2017)

We report a detailed study of the transport properties of a β-Bi_4I_4 quasi-one-dimensional topological insulator. Electrical resistivity, thermoelectric power, thermal conductivity, and Hall coefficient measurements are consistent with the possible appearance of a charge-density-wave order at low temperatures. Both electrons and holes contribute to the conduction in β-Bi_4I_4 and the dominant type of charge carrier changes with temperature as a consequence of temperature-dependent carrier densities and mobilities. Measurements of resistivity and Seebeck coefficient under hydrostatic pressure up to 2 GPa show a shift of the charge-density-wave order to higher temperatures suggesting a strongly one-dimensional character at ambient pressure. Surprisingly, superconductivity is induced in β-Bi_4I_4 above 10 GPa with T_c of 4.0 K which is slightly decreasing upon increasing the pressure up to 20 GPa. Chemical characterization of the pressure-treated samples shows amorphization of β-Bi_4I_4 under pressure and rules out decomposition into Bi and BiI_3 at room-temperature conditions.

DOI: 10.1103/PhysRevB.95.235149

I. INTRODUCTION

In the last years several bismuth binary compounds have been rediscovered as topological insulators (TIs) [1,2]. In TIs metallic surface states coexist with the bulk band gap as a result of strong spin-orbit coupling. These surface states are topologically protected, which implies that they can be hardly altered by impurities or crystal defects, and exhibit unique transport phenomena [3]. We recently reported the discovery of a quasi-one-dimensional (quasi-1D) topological insulator in bismuth iodide β-Bi_4I_4 [4]. The crystal structure of β-Bi_4I_4 is composed of narrow one-dimensional metallic bismuth stripes that extend along the b crystallographic axis [5–7]. These 1D building blocks are held together by weak noncovalent bonds, forming two-dimensional (2D) layers parallel to each other that in turn pile up making a three-dimensional (3D) bulk crystal structure [5–7]. High anisotropy of the quasi-one-dimensional crystal structure manifests itself also in the needlelike shape of β-Bi_4I_4 single crystals. Both first-principles electronic structure calculations and angle-resolved photoemission spectroscopy (ARPES) studies demonstrate that β-Bi_4I_4 is at the boundary between a strong-weak topological insulator phase and a trivial insulator [4]. Pressure or chemical doping could drive the material in one or the other phase inducing a topological phase transition [4,8] as already observed in β-As_2Te_3 [9] and PbTe [10]. Moreover, pressure can efficiently modify the small band gap and the band structure of TIs, enhancing the thermoelectric properties, without introducing additional disorder as chemical doping would do [11].

In this work, we report the temperature dependence of resistivity, thermoelectric power, thermal conductivity, and Hall coefficient of β-Bi_4I_4 single crystals. Resistivity and thermoelectric power were measured as a function of temperature under hydrostatic pressure up to 2 GPa. Measurements of the electrical resistivity in quasihydrostatic pressure up to 20 GPa reveal that superconductivity emerges in β-Bi_4I_4 above 10 GPa. Chemical stability of pressure-treated β-Bi_4I_4 crystals was studied at various temperatures by means of x-ray powder and single-crystal diffraction and energy-dispersive x-ray analysis.

II. EXPERIMENTAL DETAILS

Single crystals of β-Bi_4I_4 were obtained by a chemical transport reaction method employing bismuth metal and HgI_2 as starting materials as described in detail in Refs. [4–6]. The obtained crystals are needle shaped with dimensions up to $10 \times 1 \times 0.5$ mm. Their high quality in terms of crystal structure and chemical composition was confirmed by the same palette of different characterization methods as in Ref. [4]. Powder samples for combined pressure-temperature treatment were synthesized following Ref. [6].

The electrical resistivity (ρ) was measured as a function of temperature along the propagation direction of the bismuth stripes (b axis) of β-Bi_4I_4 single crystals, in a conventional four-point configuration using a delta-mode technique to eliminate thermoelectric voltages. Gold wires were attached to the samples by means of a graphite-based glue. For the measurement of thermoelectric power (S) the sample was placed on an electrical insulating ceramic bar, with a small heater anchored at one end. The heat generated by the small resistor propagated through the sample along the b axis while the temperature gradient across it was measured by a differential type-E thermocouple, as described elsewhere [12]. To avoid any undesired reaction between the sample and air moisture, the resistivity and thermoelectric power measurements, at ambient pressure, were performed in helium gas atmosphere. The thermal conductivity (κ) of β-Bi_4I_4 single crystals was measured by a steady-state method under vacuum (base pressure of 10^{-6} mbar) along the b axis direction [13]. A small chip resistor was directly glued on one side of the sample using Stycast FT 2850. In order to measure the amount of heat passing through the specimen, a stainless steel reference sample of known thermal conductivity was connected between the sample and the copper sample holder, which acted as a heat

*andrea.pisoni@epfl.ch

sink. The temperature gradient on the reference sample and on the crystal was measured by type-E differential thermocouples. A temperature gradient of 1 K was carefully maintained across the sample at all temperatures. To measure the Hall coefficient (R_H) a thin single crystal of β-Bi_4I_4 was shaped into a standard six-terminal Hall bar configuration by the focused ion beam (FIB) technique. Platinum leads were deposited on the sample by FIB. R_H was measured applying a magnetic field of 1 T, perpendicular to the sample's b axis direction, that was reversed to eliminate the contribution from misaligned Hall contacts.

The temperature dependences of ρ and S were measured simultaneously on the same sample under hydrostatic pressure up to 2 GPa provided by a piston-cylinder cell employing Daphne oil 7373 as a pressure transmitting medium. The pressure was determined by the superconducting transition temperature of a lead pressure gauge. The electrical resistivity under high pressure was extended up to 20 GPa in a diamond anvil cell (DAC). For this scope electrical leads were implanted in the diamond culet by FIB and the sample was directly pressed on them during the measurement. Rhenium metal was used for the gasket, that was insulated from the platinum leads by a mixture of fine Al_2O_3 powder and black Stycast 2850 FT. NaCl powder was used as a pressure transmitting medium. The pressure was measured at room temperature from the shift of the fluorescence line of a small ruby grain placed close to the sample [14].

After pressure release the sample with the transmission medium was extracted from the gasket hole and the diffraction data were taken from the rotating sample at ID23 ESRF beamline using $\lambda = 0.6888$ Å wavelength at 173 K. A PILATUS 6M detector was used; frames were binned by SNBL TOOL BOX software [15] and azimuthal integration was done using FIT2D [16]. Afterwards the chemical composition of the crystal was identified by energy-dispersive x-ray analysis (EDX). The spectra were collected using Oxford Silicon Drift X-Max^N detector at an acceleration voltage of 20 kV and a 100 s accumulation time. The EDX analysis was performed using the *P/B-ZAF* reference-free method (where Z = atomic number correction factor, A = absorption correction factor, F = fluorescence factor, P/B = peak to background model). Scanning electron microscopy (SEM) was performed on a SU8020 (Hitachi) with a photodiode-low-energy-backscattered-electrons detector to obtain evaluable Z contrast ($U_a = 3$ kV).

Additionally, a series of compression experiments on presynthesized β-Bi_4I_4 polycrystalline powders and selected single crystals were performed in a multianvil device at different temperatures (from room temperature up to 1273 K) and pressures (from 2 to 10 GPa) with different exposure times (from 30 to 270 min). For all experiments, Bi_4I_4 samples were filled into a molybdenum capsule (0.025 mm foil, 99.95%, Alfa Aesar, Karlsruhe, Germany). The capsule was transferred into a crucible made of hexagonal boron nitride (HeBoSint® P100, Henze BNP GmbH, Kempten, Germany), built into an 18/11 assembly, and compressed by eight tungsten carbide cubes (HA-7%Co, Hawedia, Marklkofen, Germany). Further information on the construction of the assembly can be found in [17–20]. To apply pressure, a hydraulic press (mavo press LPR 1000-400/50, Max Voggenreiter GmbH, Mainleus, Germany) and a modified Walker-type module (also Max Voggenreiter GmbH) were used. Depending on the requested pressure, compression and decompression lasted from 60 to 240 and 180 to 700 min, respectively. Additional heating was applied during the interjacent exposure time. Crystallinity and phase composition of these samples were studied by x-ray powder diffraction [Stoe Stadi P powder diffractometer with Ge(111) monochromatized Mo $K\alpha_1$ ($\lambda = 70.93$ pm) radiation equipped with a Mythen 1K detector].

III. RESULTS AND DISCUSSION

A. Ambient pressure transport properties

Figure 1(a) presents the electrical resistivity of β-Bi_4I_4 measured in the 4–300 K temperature range, in logarithmic scale. Three different regimes can be identified: for temperatures above 150 K β-Bi_4I_4 displays semiconducting behavior ($d\rho/dT < 0$), while at lower temperatures $\rho(T)$ starts decreasing smoothly down to 80 K, where a sharp insulating transition increases its value by one order of magnitude. As T further decreases another mild change of slope appears around 50 K. The fitting of $\rho(T)$ for $T > 150$ K with a thermally activated model $\rho(T) = \rho_0 \exp(\Delta/k_B T)$ (where Δ is the activation energy and k_B the Boltzmann constant) gives a value of $\Delta = 36$ meV [inset of Fig. 1(a)], as we already reported [4]. This value is astonishingly close to that of the small direct band gap at the Y point of the bulk Brillouin zone estimated by the GW calculations [4]. In order to check the reproducibility of our results, we measured $\rho(T)$ of another five β-Bi_4I_4 single crystals with various dimensions. These results are presented in different colors in Fig. 1(b). The resistivity curves are normalized to their value at 300 K to emphasize the high-temperature region. As can be seen, the different curves overlap perfectly at high temperatures indicating the same value of Δ. Filatova *et al.* [6] suggested that the steep increase of $\rho(T)$ around 80 K could be caused by a charge-density-wave (CDW) transition in β-Bi_4I_4: In fact the quasi-1D character of this compound would facilitate the appearance of such ordered state. In order to investigate the assumed CDW transition we plotted the derivatives of the logarithm of the different renormalized resistivity curves, $d(\ln \rho^*)/d(1/T)$ [where $\rho^* = \rho(T)/\rho(300\,\mathrm{K})$], as a function of T [inset in Fig. 1(b)]. A sharp peak around $T^{\rho}_{CDW} \sim 80$ K is clearly visible in the derivative of the different curves, very similarly to what was observed in other CDW materials [21]. The value of T^{ρ}_{CDW} does not appear to change significantly between the samples. However, the flattening of the resistivity curve at lower temperature is more or less pronounced and occurs at different temperatures in different samples, suggesting that it could be caused by shallow in-gap impurity levels.

The thermal conductivity of β-Bi_4I_4 (Fig. 2) has a value of $\kappa\,(300\,\mathrm{K}) = 22\,\mathrm{W\,K^{-1}\,m^{-1}}$, that is very high for a quasi-1D material and it is even higher than that of bulk Bi_2Te_3 ($\sim 2\,\mathrm{W\,K^{-1}\,m^{-1}}$ [22]) and BiTeCl ($\sim 3\,\mathrm{W\,K^{-1}\,m^{-1}}$ [23]). At high temperature κ decreases monotonically down to a broad minimum around 135 K, below which it recovers the temperature dependence predicted by the Callaway theory [13,24]. On a general basis, the total κ is composed of an electrical and a phononic contribution. Similar to other poorly conducting

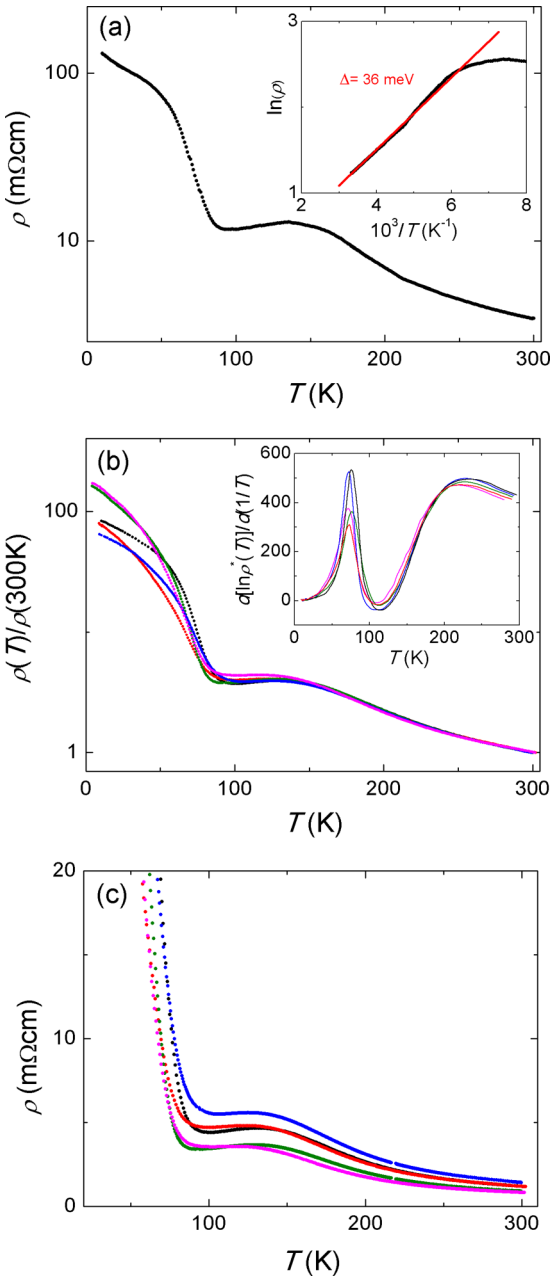

FIG. 1. (a) Temperature-dependent resistivity of a β-Bi_4I_4 single crystal. The inset shows the logarithm of the resistivity as a function of inverse temperature. The fitting of the curve with a thermally activated model (red line) gives an activation energy (Δ) of 36 meV. (b) Temperature dependence of the resistivity of other five β-Bi_4I_4 single crystals normalized to the value at 300 K in order to emphasize the high-temperature region. These different curves overlap very well, indicating the same value of the thermal activation energy, as described in the text. The inset presents a comparison between the derivatives of the logarithm of the different renormalized resistivity curves as a function of temperature. The peak position attributed to the assumed CDW transition (T^{ρ}_{CDW}) does not notably change between the different samples. (c) Temperature-dependent resistivity of the five β-Bi_4I_4 single crystals shown in (b) on the linear scale.

materials, we can expect that the dominant contribution to κ in β-Bi_4I_4 is given by phonons [21]. Indeed, assuming an electron density that justifies the usage of the Wiedemann-Franz law,

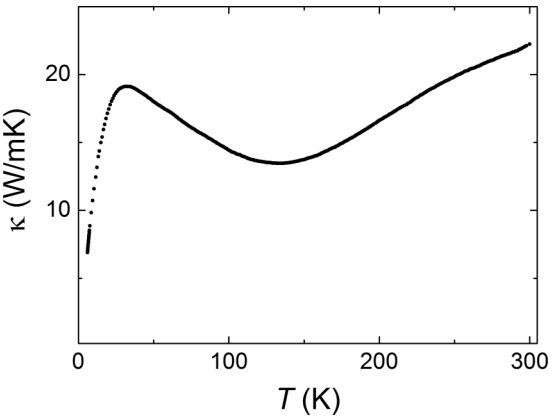

FIG. 2. Temperature dependence of the thermal conductivity of a β-Bi_4I_4 single crystal. The broad minimum corroborates the presence of a CDW order.

one estimates the thermal conductivity due to charge carriers lower than 1 W K^{-1} m^{-1}. Therefore, one can safely neglect this term and analyze the behavior of κ in terms of purely phononic contribution. Within this frame, one would expect an increase with decreasing temperature for a highly crystalline solid. The opposite, very unusual feature indicates that there are other degrees of freedom which strongly scatter the phonons and decrease. In our description, fluctuating CDWs (which through the electron-phonon coupling causes fluctuation of lattice positions) are at the origin of this behavior. Once they order three dimensionally, this source of phonon scattering disappears and it starts to increase in a standard manner. However, this increase is not very sharp, not like in 1T-$TaSe_2$ [25] which raises questions about the correlation length of the CDW. Nevertheless, at this point this temperature dependence is the strongest indication for the existence of CDWs in this material. The maximum that appears around 32 K is a consequence of the size effect. At very low temperatures, only the long-wavelength phonons remain in the system, which are constrained by the sample dimensions and their heat transport becomes less efficient on cooling down.

A striking feature of κ is the linear decrease at high T which is quite unusual for a highly crystalline sample. It could be considered as a sign of CDW fluctuations which diffuse the phonons. When a long-range CDW order establishes, this source of scattering disappears and κ follows the T dependence expected for crystalline solids. It has to be mentioned that the T^{ρ}_{CDW} is identified at around 80 K, but κ starts to increase slightly already at 100 K. It means that built-up interchain CDW correlations are already sufficient for decrease in phonon scattering. Very similar observations were reported in other CDW compounds such as 2H-$TaSe_2$ [25], $(NbSe_4)_3I$, and $K_{0.3}MoO_3$ [26]. The significant difference between the CDW transition temperature observed in $\rho(T)$ and in $\kappa(T)$ can be explained by fluctuation effects. Specific heat measurements on $K_{0.3}MoO_3$ demonstrated that fluctuation effects can appear above T_{CDW} over a temperature interval that can be as wide as 30 K [27].

Both the negative Seebeck [Fig. 3(a)] and the Hall [Fig. 3(b)] coefficients confirm that electrons are the dominant type of charge carriers in β-Bi_4I_4 at high temperature. Upon

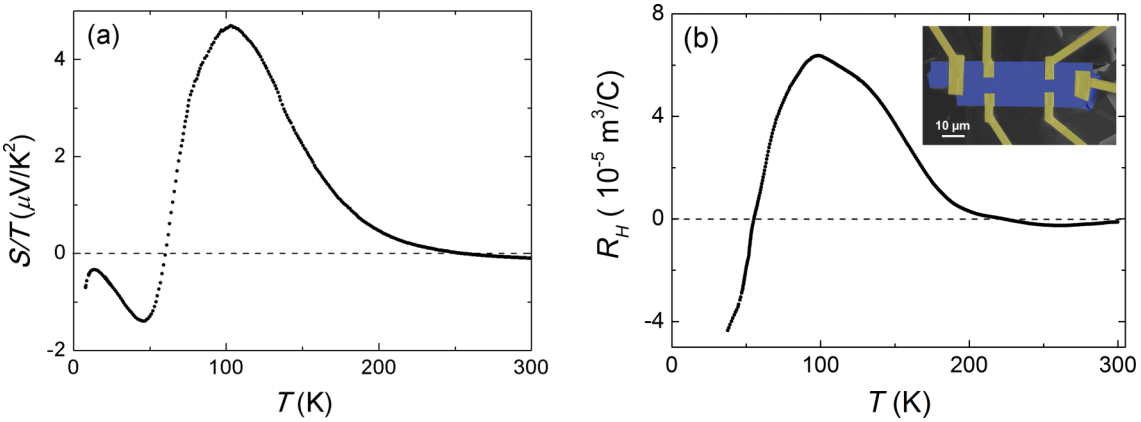

FIG. 3. (a) Ratio between thermoelectric power of a β-Bi_4I_4 single crystal and temperature plotted against temperature. (b) Temperature-dependent Hall coefficient of a β-Bi_4I_4 single crystal. The inset shows a SEM image of the sample fabricated by FIB and contacted in a Hall bar configuration. The sample is highlighted in blue and the deposited electrical contacts in yellow.

decreasing T, the increment in S/T and R_H becomes positive below 260 and 230 K, respectively. This indicates that, indeed, both electrons and holes contribute to the electrical conduction in β-Bi_4I_4. The thermoelectric power and the Hall coefficient for a nondegenerate semiconductor in a two-band model, consisting of electron and hole bands, can be expressed as [27,28]

$$S(T) = -\frac{k_B}{e}\left(\frac{\mu_e - \mu_h}{\mu_e + \mu_h}\right)\left(\frac{\Theta}{k_B T} + \text{constant}\right), \qquad (1)$$

and

$$R_H = \frac{1}{e}\frac{n_h\mu_h^2 - n_e\mu_e^2}{(n_h\mu_h + n_e\mu_e)}, \qquad (2)$$

where e is the electron charge, $\mu_e(\mu_h)$ is the electron (hole) mobility, $n_e(n_h)$ is the electron (hole) density, and Θ is the activation energy (in principle different from Δ). Equations (1) and (2) successfully describe the temperature dependence of S and R_H as the balance between the hole and electron bands being changed by T-dependent mobilities and carrier density if the charges respond differently to phonons or charge fluctuations. Unfortunately, without additional insight, there is no sense in determination of $\mu_e(\mu_h)$ and $n_e(n_h)$. Knowing the transport coefficients, ρ, S, and κ, one can calculate the dimensionless thermoelectric figure of merit, $ZT = \frac{S^2}{\rho\kappa}T$. Values of $ZT \geqslant 1$ are required for materials promising for thermoelectric applications [29]. β-Bi_4I_4 possesses $ZT(300\,\text{K}) = 4 \times 10^{-4}$ that increases only to 1.8×10^{-2} at 125 K where its maximum appears. Below this temperature ZT decreases further. These values render β-Bi_4I_4 unfavorable for thermoelectric applications [29], which is not surprising given the high values of thermal conductivity and electrical resistivity.

B. Pressure effect

The temperature dependence of the electrical resistivity measured under hydrostatic pressure up to 2 GPa is shown in Fig. 4(a). Hydrostatic pressure (p) monotonously increases the resistivity at room temperature from $\rho(300\,\text{K}) = 3\,\text{m}\Omega\,\text{mm}$ at ambient pressure to $38\text{m}\Omega\,\text{mm}$ at 2 GPa and shifts the local maximum in ρ to higher temperatures. In order to study the effect of pressure on the CDW transition, we plotted $d(\ln\rho)/d(1/T)$ as a function of T for different pressures [Fig. 4(b)]. The CDW transition temperatures at different pressures can be clearly identified as the temperatures where a peak in the derivative occurs. The inset of Fig. 4(b) presents the pressure dependence of T^{ρ}_{CDW}. With increasing pressure the height of the peaks in Fig. 4(b) is greatly reduced. This could indicate that pressure weakens the CDW transition in β-Bi_4I_4, in good agreement with the general trend reported for other CDW materials [30,31]. At first sight, the monotonous increase of T^{ρ}_{CDW} with pressure seems to contradict the previous conclusion. A similar enhancement of the CDW transition temperature by pressure was already observed in $(NbSe_4)_{10/3}I$ [32], $(TaSe_4)_2I$ [33], and in some organic charge-transfer salts [34]. A tentative explanation of this observation is the following: in quasi-1D systems T^{ρ}_{CDW} is a function of dimensionality, e.g., of the interchain coupling [35], and pressure can cause an increase of T^{ρ}_{CDW} by suppressing the 1D fluctuations both directly or indirectly [33]. In an ultimate 1D system a CDW ordering would be impossible because large fluctuations preclude any long-range order, while in a 3D system, by definition, there is no 1D phase transition. Consequently, there should be a maximum in $T^{\rho}_{\text{CDW}}(p)$ depending on the interchain coupling (degree of one dimensionality). It appears from our measurements that our system is on the one-dimensional side of $T^{\rho}_{\text{CDW}}(p)$, and pressure is bringing it to the maximum value of T^{ρ}_{CDW} but without reaching it. Figure 4(c) shows the evolution of the thermal activation energy, extracted from ρ at high temperature, as a function of pressure for two different samples. The measurement of Δ under pressure is particularly important because first-principles calculations [4] predict a vanishing band gap at a critical pressure value that would correspond to a possible topological phase transition between strong and weak topological insulator phases. However, we have not observed it in the 0–2 GPa pressure range.

The temperature dependence of the Seebeck coefficient is already very complex at ambient pressure and it remains as such at different pressures [Fig. 3(b)]. We suppose that it reflects changes in the subtle balance among the contributions of two types of carriers upon variations of temperature and

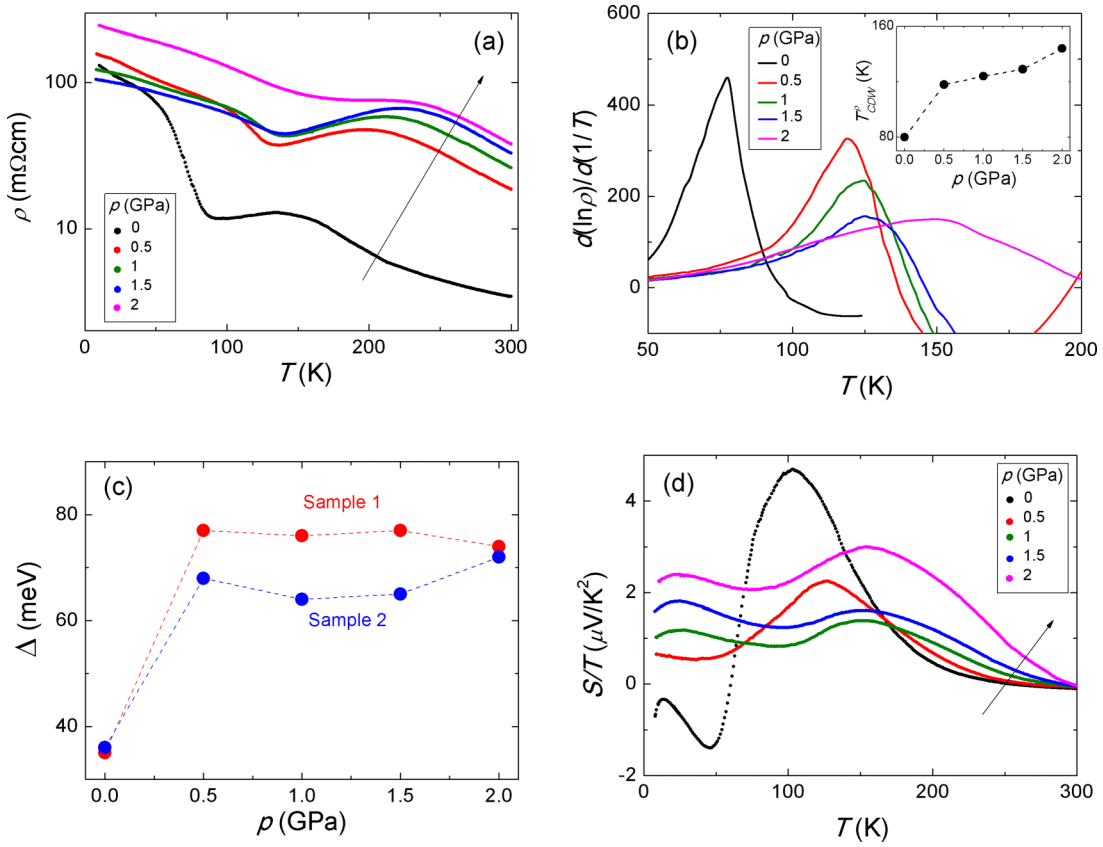

FIG. 4. (a) Electrical resistivity of β-Bi_4I_4 as a function of temperature, measured at different pressures. Increase in pressure is indicated by the black arrow. (b) The derivative of the logarithmic electrical resistivity of β-Bi_4I_4 measured at different pressures and plotted against T, at low temperatures. The temperature at which the peak occurs in the different curves marks the CDW phase transition temperature T^{ρ}_{CDW}. The inset presents the pressure dependence of T^{ρ}_{CDW}, the black dashed line is a guide to the eye. (c) Pressure dependence of the thermal activation energy extracted from resistivity measurements of two different samples. The results appear quite reproducible. Colored dashed lines are a guide to the eye. (d) Temperature dependence of the thermoelectric power of β-Bi_4I_4 measured at different pressures. The pressure increases along the black arrow.

pressure. Pressure induces only a small change in $S(300\,\mathrm{K})$ that becomes less negative. The main changes are visible in the temperature (T^{S}_{max}) and the magnitude (S_{max}) of the maximum of S. Pressure pushes T^{S}_{max} towards higher temperatures in the same way as T^{ρ}_{CDW}. This confirms that the maximum of S is somehow related to the appearance of the CDW state. The value of S_{max} first decreases from 505 μV/K at 0 kbar to 218 μV/K at 10 kbar, and for higher pressures it increases again reaching a value of 495 μV/K at 20 kbar. The abrupt increase of S_{max} at 20 kbar could be associated with the less conducting behavior of $\rho(T)$ at the same pressure. Below 50 K the Seebeck coefficient changes the sign moving from negative to positive above 5 kbar. S remains positive with further increasing p, and the slope at which it approaches zero increases. This indicates that holes become the dominant charge carriers in β-Bi_4I_4 for $p > 5$ kbar at low temperature.

C. Pressure-induced superconductivity

Superconductivity was induced in β-Bi_4I_4 under quasihydrostatic pressure provided by a diamond anvil cell (DAC). The temperature-dependent resistance of a β-Bi_4I_4 single crystal at various pressures up to 20 GPa is shown in Fig. 5(a). The overall behavior resembles the cases of $ZrTe_5$ three-dimensional topological insulator recently published by Zhou *et al.* [36] and of the Rashba-material BiTeI that undergoes a topological transition under pressure as discovered by various groups [37–39]. The β-Bi_4I_4 sample was mechanically pressed on the electrical contacts, and for this reason it was not possible to measure it at pressures lower than 5 GPa. Already at 5 GPa the resistance shows a T dependence strongly differing from the observations at 2 GPa in Fig. 4(a). At high T some reminiscent insulating behavior can still be noticed and the slope of $R(T)$ decreases around 150 K. At $p \geqslant 8$ GPa, $R(T)$ presents an almost temperature-independent behavior that is most likely the result of a pronounced pressure inhomogeneity. The value of R (300 K) does not follow a monotonic trend: At first it increases up to $p = 10$ GPa and then noncontinuously decreases at $p > 10$ GPa. These two observations, especially the almost temperature-independent resistivity which would correspond to a high level of static disorder, may indicate that the sample lost its crystallinity under pressure.

This has fingerprints in the appearance of superconductivity with pressure, as well. Figure 5(b) shows the resistance curves normalized to their value at 10 K to emphasize the change in the critical temperature (T_c) as a function of pressure. A superconductivity onset is observed around 4 K at 10 GPa. In the following analysis we define T_c^{onset} as the temperature

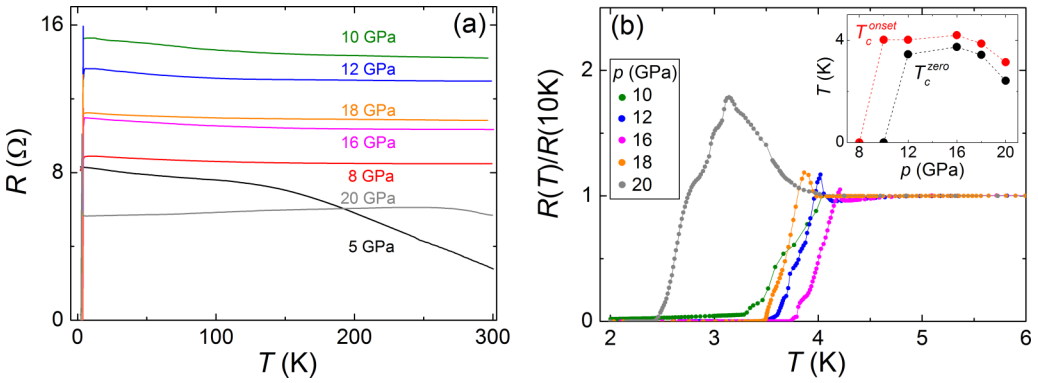

FIG. 5. (a) Temperature dependence of the resistance of a β-Bi_4I_4 single crystal measured at high pressure. (b) Detailed view of the resistance curves normalized to their value at 10 K in order to emphasize the change in T_c as a function of pressure. The inset shows the pressure dependence of the onset temperatures and zero-resistance critical temperatures.

extracted from the intersection of two linear fits: one drawn in the normal state just above the superconducting transition and one in the steepest part of the transition. For $p > 10$ GPa we identify T_c^{onset} with the temperature of the peak appearing just above the superconducting transition. Moreover, we define T_c^{zero} as the temperature at which $R(T) \sim 0$, namely, when $R(T)$ falls below the limit of sensitivity of our instruments. At 10 GPa, $R(T)$ does not approach zero, presumably indicating a filamentary type of superconductivity. At 12 GPa, the zero-resistance state sets off and persists up to 20 GPa. Already at 12 GPa we observe a sharp peak appearing just above the transition which is the fingerprint of the nonuniformity of the superconductivity. Furthermore, some steps can be seen in the drop of $R(T)$, although the superconducting transition width is always less than 1 K for all applied pressures. These could be caused by inhomogeneity of the pressure distribution over the sample. The inset in Fig. 4(b) shows the pressure dependences of T_c^{onset} and T_c^{zero}. The T-p phase diagram presents a nice domelike structure suggesting an optimum $T_c^{onset} \sim 4.2$ K at 16 GPa, that decreases to 3.2 K at 20 GPa. We were able to tune T_c of β-Bi_4I_4 reversibly by increasing and decreasing pressure up to 20 GPa. Proximity of the assumed CDW and the superconducting order could create a fascinating scenario where the rapid rise of the CDW transition upon increasing pressure below 2 GPa and its fall at pressures above 5 GPa yields $T_{CDW} = 0$ in the range where superconductivity is observed. Consequently, this situation would suggest that superconductivity appears because of a CDW quantum critical point.

D. Chemical characterization of the pressure-treated samples

The observed T-independent resistivity and the inhomogeneities seen in the superconducting transition predicated a study of pressure-dependent chemical stability of β-Bi_4I_4. Three possible scenarios of chemical alternation were taken into account: amorphization of β-Bi_4I_4, structural transition between β-Bi_4I_4 and α-Bi_4I_4 modifications of the bismuth monoiodide, and decomposition into elemental bismuth and BiI_3 which occurs at ~603 K [40] at ambient pressure. Particularly, the last instance would be discouraging since amorphous bismuth precipitates could then support superconductivity [41,42]. The critical temperature T_c of the elemental bismuth is 7 K at 5 GPa and slightly decreases upon increasing pressure [42]. Hence the discrepancy observed in our experiments (4 K vs 7 K) could be in principle ascribed to a size effect of Bi particles. BiI_3, which would be the other decomposition product in this case, is fairly air sensitive and would lead to rapid hydrolysis and oxidation of the sample in air. The resistivity of BiI_3 under pressures up to 3.3 GPa was recently studied elsewhere [43].

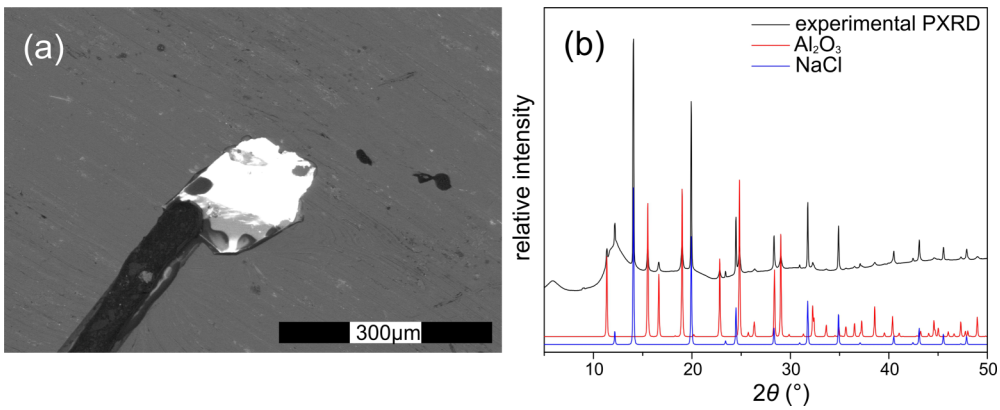

FIG. 6. (a) Bismuth monoiodide crystal after the pressure treatment at 20 GPa (SEM micrograph, 3 kV, PD-BSE detector). (b) Corresponding synchrotron x-ray diffraction pattern.

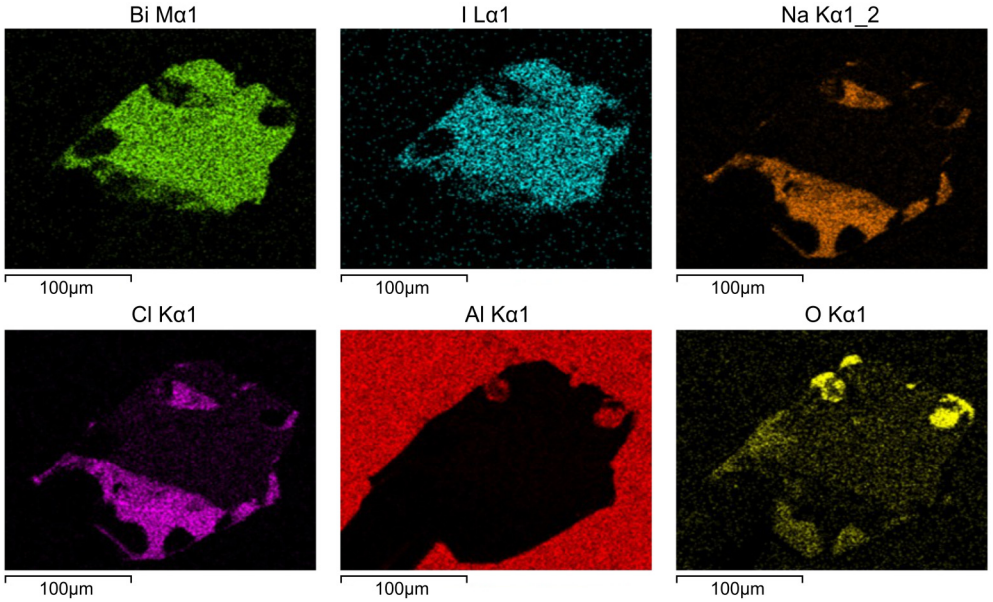

FIG. 7. EDX mapping spectra for the β-Bi_4I_4 crystal after high-pressure treatment (first measurement; see text). Note distinct areas corresponding to admixtures of NaCl and Al_2O_3. The accuracy of the composition determination was enhanced thanks to NaCl acting as an internal reference. Averaged results of the first measurement: Bi 47.4 at. %, I 52.6 at. %; Na 53.0 at. %, Cl 47.0 at. %. Averaged results of the second measurement (performed after 7 months): Bi 48.0 at. %, I 52.0 at. %; Na 53.3 at. %, Cl 46.7 at. %.

First and foremost, the sample treated at 20 GPa was analyzed via a synchrotron x-ray diffraction measurement performed at the European Synchrotron Radiation Facility (ESRF). Regardless of the obvious physical integrity of the sample and its smooth surface without signs of deterioration [Fig. 6(a)], all observed Bragg reflections could be assigned to ruby (Al_2O_3) and NaCl only, thus hinting at amorphization of bismuth monoiodide under pressure [Fig. 6(b)]. One could argue that the small bump in the diffraction pattern at about 9° of 2θ (note the wavelength of 0.6888 Å) can be attributed to the periodicity of a single one-dimensional bismuth stripe. The respective recalculated d spacing of ∼4.4 Å accords well with the unit cell parameter b of the crystalline β-Bi_4I_4 that in turn corresponds to the length of one linkage of the bismuth-iodine stripe. In an amorphous sample which contains disordered one-dimensional stripes this would be indeed the only possible repeat distance, an indication of short-range ordering. It should be noted that the respective (010) reflection is not observed in the diffraction pattern of pure crystalline β-Bi_4I_4 due to the reflection conditions of the space group ($C2/m$).

Two consecutive EDX analyses of the sample (with a time interval of 7 months) confirmed very uniform distribution of bismuth and iodine with the ratio close to 1:1 in both measurements (Fig. 7). The surface appears moderately oxidized, thus

TABLE I. Conditions for pressure experiments and identified products.

Pressure (GPa)	Temperature (K)	Compression/decompression time (min)	Exposure time (min)	Identified phases
		Single crystals		
3	473	70/210	70	α-, β-Bi_4I_4
3	623	70/210	70	α-, β-Bi_4I_4, Bi, BiI_3
5	1023	130/365	270	Bi, BiI_3
7.5	293	210/600	30	α-, β-Bi_4I_4
7.5	293	210/600	180	α-, β-Bi_4I_4
10	443	235/700	70	Bi, BiI_3
10	553	235/700	85	Bi, BiI_3
		Powdered samples		
2	873	60/180	80	Bi, BiI_3
3	453	70/210	65	α-, β-Bi_4I_4
3	573	70/210	65	α-, β-Bi_4I_4
5	573	130/365	120	α-, β-Bi_4I_4, Bi, BiI_3
5	673	130/365	90	Bi, BiI_3
5	1023	130/365	210	Bi, BiI_3
5	1273	130/365	65	Bi, BiI_3
7.5	523	210/600	100	Bi, BiI_3

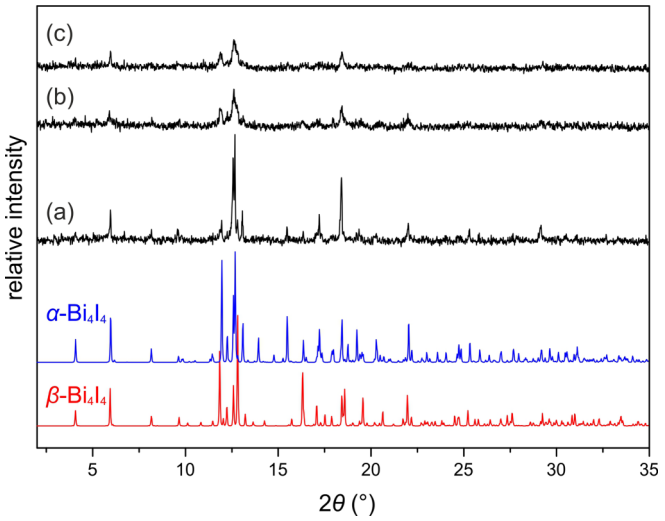

FIG. 8. A PXRD study (collected on Mo Kα radiation) showing the impact of high-pressure treatment on bismuth monoiodide crystals at room temperature: (a) starting material; (b) the same sample exposed to 7.5 GPa for 30 min; (c) the same sample exposed to 7.5 GPa for 180 min.

ruling out any significant admixtures of BiI_3. The presence of any Bi crystallites was not observed. These results support that at least the chemical composition of Bi_4I_4 is preserved and thus an amorphous phase of Bi_4I_4 could support superconductivity, for instance, as in some amorphous actinide alloys [44]. This possibility is very interesting by itself, and it could be the subject of an upcoming study.

Furthermore, pressure- and temperature-induced effects on structure and composition of the starting material β-Bi_4I_4 were studied on larger amounts of presynthesized well-crystalline samples using the multianvil technique. These experiments are summarized in Table I. Experiments at room temperature and 7.5 GPa with different exposure times (30 and 180 min, respectively) reveal time-dependent amorphization of the sample (see the results of x-ray powder diffraction measurements in Fig. 8). The reflection intensities drop significantly with increasing exposure time. No indication of formation of other decomposition products was found. As no *in situ* measurements were carried out during these experiments, it was not possible to make a statement as to whether pressure-induced amorphization of Bi_4I_4 took place or whether an amorphous decomposition product of an intermediate phase, which is unstable at ambient pressure, had formed.

Further multianvil experiments at different pressures (2, 3, 5, 7.5, and 10 GPa) and an energy input in the form of heating (from 443 to 1273 K) revealed a decomposition of Bi_4I_4 into Bi and BiI_3 at 7.5 GPa and above, whereas between 2 and 5 GPa, a mixture of β-Bi_4I_4 and α-Bi_4I_4 survived the annealing at temperatures below ~623 K showing a strong tendency towards rapid amorphization.

Also at higher temperatures (T = 673–1273 K), decomposition in Bi and BiI_3 took place in the pressure range of 2–5 GPa. Furthermore, BiI_3 needle-shaped crystals could be grown at all the above-mentioned pressures and temperatures between 973 and 1273 K.

IV. CONCLUSIONS

We investigated the transport properties of the quasi-one-dimensional β-Bi_4I_4 single crystals. Electrical resistivity, thermoelectric power, thermal conductivity, and Hall coefficient reveal a very rich temperature dependence which is tentatively ascribed to CDW formation. Seebeck and Hall coefficients show that both electrons and holes contribute to the conduction in β-Bi_4I_4 and that the dominant type of charge carriers changes with temperature as a consequence of changes in the mobilities and densities of the two types of carriers. Application of hydrostatic pressure up to 2 GPa shifts the CDW transition in β-Bi_4I_4 to higher temperatures, as demonstrated by resistivity and thermoelectric power measurements. Resistivity measurements up to 20 GPa reveal that superconductivity is induced in β-Bi_4I_4 at 10 GPa although the material loses its crystallinity and retains its composition. A maximum critical temperature of 4.2 K is reached at 16 GPa, which decreases slightly upon further increase of pressure. Decomposition of β-Bi_4I_4 into Bi and BiI_3 occurs in the 2–7.5 GPa range only at elevated temperatures. Despite this detailed study of the transport coefficients we could not pinpoint a particular property which would be typical for the topological insulating nature of β-Bi_4I_4 reported previously.

ACKNOWLEDGMENTS

This work was supported by the Swiss National Science Foundation (Project No. 200021_138053) and by the German Research Foundation (DFG) in the framework of the Special Priority Programme (SPP 1666) "Topological Insulators" (DFG Project No. IS 250/1-1) and by the ERA-Chemistry Programme (DFG Project No. RU 776/15-1 and FWF Project No. I 2179). G.A. and O.V.Y. acknowledge support by the NCCR Marvel and the European Research Council (ERC) Starting grant "TopoMat" (Grant No. 306504). We are grateful to Dr. Alexey Bosak (ESRF, Grenoble, France) for the synchrotron measurements of our sample and to Professor Michael Ruck, Mr. Alexander Weiz, and Mrs. Michaela Munch (TU Dresden, Germany) for valuable discussions and assistance in synthesis.

[1] Y. Xia, D. Qian, D. Hsieh, L. Wray, A. Pal, H. Lin, A. Bansil, D. Grauer, Y. S. Hor, R. J. Cava, and M. Z. Hasan, Nat. Phys. **5**, 398 (2009).

[2] H. Zhang, C.-X. Liu, X.-L. Qi, X. Dai, Z. Fang, and S.-C. Zhang, Nat. Phys. **5**, 438 (2009).

[3] C. Shekhar, C. E. ViolBarbosa, B. Yan, S. Ouardi, W. Schnelle, G. H. Fecher, and C. Felser, Phys. Rev. B **90**, 165140 (2014).

[4] G. Autès, A. Isaeva, L. Moreschini, J. C. Johannsen, A. Pisoni, R. Mori, W. Zhang, T. G. Filatova, A. N. Kuznetsov, L. Forró, W. Van den Broek, Y. Kim, K. S. Kim, A. Lanzara, J. D. Denlinger, E. Rotenberg, A. Bostwick, M. Grioni, and O. V. Yazyev, Nat. Mater. **15**, 154 (2016).

[5] H. G. von Schnering, H. von Benda, and C. Kalveram, Z. Anorg. Allg. Chem. **438**, 37 (1978).

[6] T. G. Filatova, P. V Gurin, L. Kloo, V. A. Kulbachinskii, A. N. Kuznetsov, V. G. Kytin, M. Lindsjo, and B. A. Popovkin, J. Solid State Chem. **180**, 1103 (2007).
[7] A. Isaeva, B. Rasche, and M. Ruck, Phys. Status Solidi RRL **7**, 39 (2013).
[8] C.-C. Liu, J.-J. Zhou, Y. Yao, and F. Zhang, Phys. Rev. Lett. **116**, 066801 (2016).
[9] K. Pal and U. V. Waghmare, Appl. Phys. Lett. **105**, 062105 (2014).
[10] P. Barone, T. Rauch, D. Di Sante, J. Henk, I. Mertig, and S. Picozzi, Phys. Rev. B **88**, 045207 (2013).
[11] K. Pal, S. Anand, and U. V. Waghmare, J. Mater. Chem. C **3**, 12130 (2015).
[12] A. Pisoni, J. Jacimovic, R. Gaál, B. Náfrádi, H. Berger, Z. Révay, and L. Forró, Scr. Mater. **114**, 48 (2016).
[13] A. Pisoni, J. Jaćimović, O. S. Barišić, M. Spina, R. Gaál, L. Forró, and E. Horváth, J. Phys. Chem. Lett. **5**, 2488 (2014).
[14] H. K. Mao, J. Xu, and P. M. Bell, J. Geophys. Res. **91**, 4673 (1986).
[15] V. Dyadkin, P. Pattison, V. Dmitriev, and D. Chernyshov, J. Synchrotron Radiat. **23**, 825 (2016).
[16] A. P. Hammersley, S. O. Svensson, M. Hanfland, A. N. Fitch, and D. Hausermann, High Press. Res. **14**, 235 (1996).
[17] D. Walker, M. A. Carpenter, and C. M. Hitch, Am. Mineral. **75**, 1020 (1990).
[18] D. Walker, Am. Mineral. **76**, 1092 (1991).
[19] D. Rubie, Phase Transitions **68**, 431 (1999).
[20] H. Huppertz, Z. Kristallogr. **219**, 330 (2004).
[21] T. Tritt, *Thermal Conductivity: Theory, Properties, and Applications* (Springer Science & Business Media, Berlin, 2005).
[22] H. J. Goldsmid, Proc. Phys. Soc. Sect. B **69**, 203 (1956).
[23] J. Jacimovic, X. Mettan, A. Pisoni, R. Gaal, and S. Katrych, Scr. Mater. **76**, 69 (2014).
[24] A. Pisoni, J. Jacimovic, O. Barišić, A. Walter, B. Nafradi, P. Bugnon, A. Magrez, H. Berger, Z. Revay, and L. Forró, J. Phys. Chem. C **119**, 3918 (2015).
[25] M. D. Núñez-Regueiro, J. M. Lopez-Castillo, and C. Ayache, Phys. Rev. Lett. **55**, 1931 (1985).
[26] A. Smontara, J. Lasjaunias, and M. Apostol, J. Low Temp. Phys. **94**, 289 (1994).
[27] R. S. Kwok, G. Gruner, and S. E. Brown, Phys. Rev. Lett. **65**, 365 (1990).
[28] H. Fritzsche, Solid State Commun. **9**, 1813 (1971).
[29] D. MacDonald, *Thermoelectricity: An Introduction to the Principles* (Courier Corporation, New York, USA, 2006).
[30] A. F. Kusmartseva, B. Sipos, H. Berger, L. Forro, and E. Tutiš, Phys. Rev. Lett. **103**, 236401 (2009).
[31] B. Sipos, A. Kusmartseva, A. Akrap, H. Berger, and L. Forró, Nat. Mater. **7**, 960 (2008).
[32] M. Petravić, L. Forró, J. R. Cooper, and F. Lévy, Phys. Rev. B **40**, 8064(R) (1989).
[33] L. Forro, H. Mutka, S. Bouffard, J. Morillo, and A. Jánossy, in *Charge Density Waves in Solids*, edited by G. Hutiray and J. Sólyom (Springer, Berlin, 1985), pp. 361–365.
[34] K. Murata, K. Yokogawa, S. Arumugam, and H. Yoshino, Crystals **2**, 1460 (2012).
[35] P. Lee, T. Rice, and P. Anderson, Phys. Rev. Lett. **31**, 462 (1973).
[36] Y. Zhou, J. Wu, W. Ning, N. Li, and Y. Du, Proc. Natl. Acad. Sci. USA **113**, 2904 (2016).
[37] D. VanGennep, A. Linscheid, D. E. Jackson, S. T. Weir, Y. K. Vohra, H. Berger, G. R. Stewart, R. G. Hennig, P. J. Hirschfeld, and J. J. Hamlin, J. Phys.: Condens. Matter **29**, 09LT02 (2017).
[38] Y. Qi, W. Shi, P. G. Naumov, N. Kumar, R. Sankar, W. Schnelle, C. Shekhar, F.-C. Chou, C. Felser, B. Yan, and S. A. Medvedev, Adv. Mater. **29**, 1605965 (2017).
[39] M. L. Jin, F. Sun, L. Y. Xing, S. J. Zhang, S. M. Feng, P. P. Kong, W. M. Li, X. C. Wang, J. L. Zhu, Y. W. Long, H. Y. Bai, C. Z. Gu, R. C. Yu, W. G. Yang, G. Y. Shen, Y. S. Zhao, H. K. Mao, and C. Q. Jin, Sci. Rep. **7**, 39699 (2017).
[40] E. V. Dikarev, V. A. Trifonov, and B. A. Popovkin, Russ. J. Inorg. Chem. **32**, 238 (1987).
[41] J. S. Shier and D. M. Ginsberg, Phys. Rev. **147**, 384 (1966).
[42] Y. Li, E. Wang, X. Zhu, and H.-H. Wen, Phys. Rev. B **95**, 024510 (2017).
[43] T. R. Devidas, N. V. Chandra Shekar, C. S. Sundar, P. Chithaiah, Y. A. Sorb, V. S. Bhadram, N. Chandrabhas, K. Pal, U. V. Waghmare, and C. N. R. Rao, J. Phys: Condens. Mater. **26**, 275502 (2014).
[44] S. Poon, A. Drehman, K. Wong, and A. Clegg, Phys. Rev. B **31**, 3100 (1985).